Identification of Motor Impairments Using Movement Distributions

BY

JOSEPH LANCASTER
B.A., Washington University in St. Louis, 2009

THESIS

Submitted as partial fulfillment of the requirements
for the degree of Master of Science in Bioengineering
in the Graduate College of the
University of Illinois at Chicago, 2015

Chicago, Illinois

Defense Committee:

James Patton, Chair and Advisor
Max Berniker, Mechanical and Industrial Engineering
Felix C. Huang, Rehabilitation Institute of Chicago

This thesis is dedicated to Beth, my wife and best friend who, despite the stress of working her way through a demanding residency in a different state, still managed to find the strength to support me in my efforts. Without her, none of this would have been possible. I love you, Beth. For keeps.

ACKNOWLEDGMENTS

I would like to thank my advisor, Dr. Jim Patton, and Dr. Felix C. Huang for years of patient guidance and generous assistance in helping me grow as a scientist, a professional, and a person. Their unwavering support and faith in me helped keep me going through the ups and downs of research, and for that I am grateful. I would also like to thank Dr. Max Berniker for his insight and suggestions for my work, as well as for serving as a member of my thesis committee.

In addition, I would like to thank all the members of the Robotics Lab at the Rehabilitation Institute of Chicago for their advice, assistance, and support; their willingness to share their ideas and lend me their time; and their welcoming attitude, which made the lab a fun and joyful place in which to work. Especial thanks are due, in no particular order, to Zachary Wright, who collected the healthy control subject data used in this study; Moria Fisher, whose knowledge and experience with grants, papers and conference presentations proved invaluable during my time as a student; Emily Lazzaro, whose insight into the practices and thoughts of physical therapists drove much of this work; Alejandro Melendez-Calderon, who taught me much of what I know about dynamic simulation of the human arm and lent me his Simulink models to build upon; and both Yazan Abdel Majeed and Justin Horowitz, who regularly offered their services as sounding boards for new ideas and consultants for problems that I struggled with.

Finally, I would like to offer my thanks to the tireless office staff of both the Rehabilitation Institute of Chicago and the Bioengineering department at the University of Illinois at Chicago. Their dedication and generosity with their time was vital in navigating the rules and documentation necessary for the submission of grants and papers, as well as attendance at conferences.

TABLE OF CONTENTS

LIST OF FIGURES

SUMMARY

A study was performed in order to determine the feasibility of identifying and quantifying motor impairment models using movement distribution data. A series of simulations of human free-exploration were systematically altered by idealized computational models of three types of motor impairments, resulting in distorted distributions in position, velocity, acceleration, angle, angular velocity, and angular acceleration space. We attempted to use these distributions to recover the impairment model parameters, called pathoparameters, which were used to generate them. Several different lookup-tables, each with a different configuration in parameter space, were generated against which to compare "unknown" test distributions. A non-negative least squares algorithm was employed to attempt to match test distributions to a combination of library distributions, allowing the estimation of the underlying pathoparameters.

It was discovered that, because the distributions for the library and test sets were generated using different base data, that there was a parameter estimation error when attempting to identify the true parameter values of a "healthy" distribution. The libraries based on a Sobol pseudo-random distribution had the lowest average error of all the library types. By comparing distributions representing a variety of types and levels of impairment, patterns of similarity were identified for future study.

It was discovered that motor impairments interact in complex, non-linear ways and, as a result, the behavior of combinations of impairments cannot be described in terms of the behavior of individual impairments. Information is needed about the entire space of possible impairment combinations in order to correctly identify the underlying pathoparameters. Even with a relatively sparse library, though, errors were comparable to the error in identification for the healthy distribution, suggesting that most of the confusion results from variability in the data used to drive the simulations. Comparison of impairment distributions revealed that direction of motion, i.e. extension vs. flexion, has the strongest impact on distribution shape, followed by joint and impairment type, respectively.

I. INTRODUCTION

It is often difficult to figure out what is wrong with patients' movement after a stroke. Motor impairments tend to be highly nonlinear and time-varying. Furthermore, clinicians tend to not all agree when they attempt to describe a pathology(Terence D Sanger et al. 2010; Terence D Sanger et al. 2006; T. D. Sanger et al. 2003; Ivanhoe and Reistetter 2004)s. One critical problem is understanding the behavioral tendencies and limitations of an individual with multiple simultaneous impairments. It is possible that this understanding can only come from a holistic analysis of multidimensional data that treats impairments as distinct, separable entities.

Assessments of motor impairment typically use an ordinal scale to describe a patient's general level of function rather than making precise, quantitative measurements of motor behaviors (Cramer, Koroshetz, and Finklestein 2007; Tsuji et al. 2000). And while there have been some calls for more quantitative assessments, clinicians continue to use these established, coarse, qualitative tools(Reuben et al. 2013). The lack of resolution in these assessments places a limit on the ability of clinicians to target therapy, and for researchers to adequately test new therapies, since these experiments typically operate with a small group of subjects over a limited timeframe (David J Gladstone, Danells, and Black 2002; D. J. Gladstone, Black, and Hakim 2002; Prange et al. 2006; Scott and Dukelow 2011). Robotic therapy, in particular, has shown some preliminary successes but the researchers studying it have had a difficult time standardizing and controlling their experiments, in part due to the nature of current assessments(Kwakkel, Kollen, and Krebs 2008).

Robotic interfaces also have the unique capacity for precision measurement and application of probing forces, including measurements and forces that would be impossible for a human therapist to produce (Figure 1). For this reason, they have been a popular tool among researchers seeking to better understand human motor control and learning (Reinkensmeyer, Emken, and Cramer 2004). But while researchers have observed changes in a subject's performances on various motor tasks with robotic interfaces, these have not translated into changes in performance scores assigned by the assessments used by clinicians(V. S. Huang and Krakauer 2009; Wolbrecht et al. 2008). Attempts have been made to use metrics only obtainable through robotic interfaces such as initial movement direction error and hand path length as proxies for impairment severity, but these have thus far only correlated weakly with the best existing clinical scales(Mostafavi et al. 2013; Scott and Dukelow 2011).

Because of this, we propose an intermediate step between the coarse, ordinal assessments given by clinicians and the abstract robotic measures that have been studied as potential correlates of those assessments. We believe that dynamic simulations of impaired movement using computational models of motor impairment may better correlate with existing clinical measures while providing insight into the nature of the impairments described in the clinical literature. The utilization of idealized models in order to investigate the specific properties of motor impairments is also advantageous in that it allows us to have complete control

over the behavior of the system. While a patient will present with an unknown variety of impairments of varying etiologies and severities, we are able to define the exact impairment model parameters, or *pathoparameters*, that we apply to the simulation. Because of this, we are able to test the feasibility of recovering or identifying these pathoparameters in a way that we would not be able to do with a human subject.

Predictive models of human movements have been well-studied for healthy individuals(Flash and Hogan 1985; Lackner and Dizio 2009). There are also some attempts at modeling pathologies such as spasticity(Le Cavorzin et al. 2001) and tremor(Sarbaz et al. 2011), but these are less common and often contentious(T. D. Sanger et al. 2003; Terence D Sanger et al. 2006). We have therefore chosen to construct new computational models designed to resemble some common motor signs associated with neurological impairments. By applying these computational models to a dynamic simulation of a two-joint arm performing free exploration, we hope to create a test-bed with which we can perform system identification on the simulation (Figure 2). In this way, we can test the feasibility of quantifying specific motor impairments using only subject behavior.

Because motor impairments might affect different kinds of movement differently, and because we are starting from a position of naïveté with respect to their characteristics, we have chosen to use a "free exploration" task to characterize the behavior associated with each of these impairments. Huang and Patton have showed that this task can be used to produce distributions that characterize individuals patients' movement patterns(F. C. Huang and Patton 2013). As such, it should be appropriate for characterizing the movement patterns associated with different motor impairments.

In this study we restrict our focus to three possible types of motor impairment models applied to a simulation of a human arm performing free exploration. Specifically, we ask if movement distributions can provide sufficient information to allow

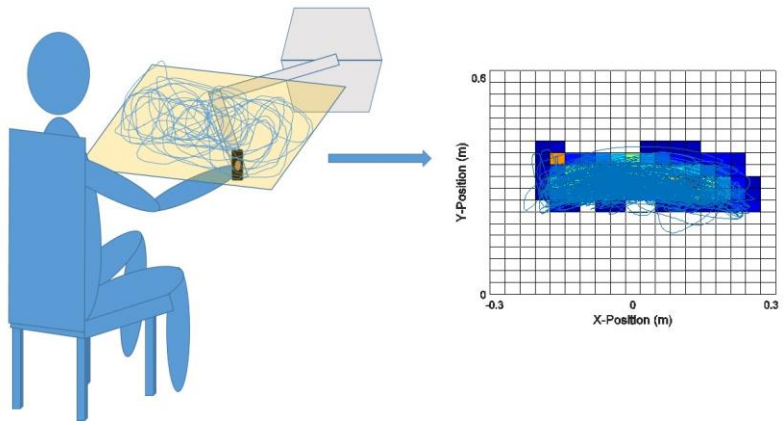

Figure 1. Free Exploration Data Converted to Distributions. Subjects performed a free exploration task while gripping a robotic interface. The resultant movements were captured electronically and represented as a distribution.

recovery of the pathoparameters by using a non-negative least squares algorithm(Chen and Plemmons 2009; D. O. Q. Lee 2012) to select a combination of impairment models from a lookup table. We hypothesize that it will be possible to approximate impairment models that do not exist in the lookup table using a combination of lookup table elements in a way that allows us to identify the underlying pathoparameters. This would be consistent with the well-known theory that human movement behaviors are built from a finite set of low-level "muscle synergies" that are scaled and shifted in time and magnitude to produce movements(d'Avella, Saltiel, and Bizzi 2003; Latash 2010).

If this is true, then the combination of models selected by the non-negative least squares algorithm should reflect the pathoparameters of the model being identified. For instance, a model comprised of spasticity and rigidity would be approximated by a combination of models from the lookup table containing spasticity and containing rigidity. If this is not the case, then a lookup-table approach will need to include models that span the space of possible impairment combinations of pathoparameters. By performing a series of repeated tests, we determine whether accurate pathoparameter recovery is possible with a variety of library structures. We also gain new knowledge about the behavior of models "corrupted" by these impairments and about the feasibility of extracting parameters from movement distributions.

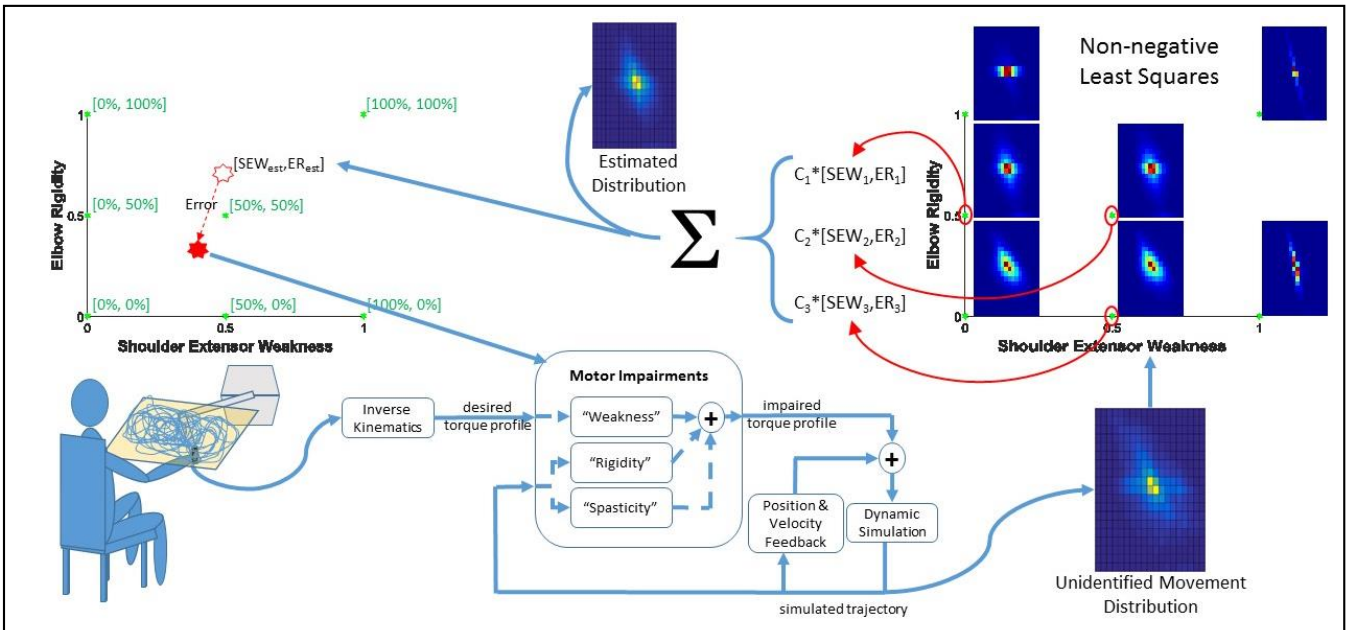

Figure 2. System Identification Using Least Squares. Healthy free-exploration data (lower left) is run through inverse kinematics to generate a feed-forward torque profile for the simulation. This torque profile is modified by the three types of impairment models (center bottom), weakness, rigidity and spasticity, before being applied to the simulated arm. This simulation results in a movement distribution (lower right), which is then compared to a library of distributions (upper right), the pathoparameters of which are known. A non-negative least squares algorithm assigns coefficients to each distribution, which we then apply to each corresponding pathoparameter set, summing the result (center). The result is a best-fit distribution (top center) and an estimated pathoparameter set (upper left), which is then compared to the actual pathoparameter set that was applied to the simulation.

II. METHODS

A. Simulations

All simulations were performed using a modified version of the arm model described by Shadmehr and Mussa-Ivaldi in 1994(Shadmehr and Mussa-Ivaldi 1994). The arm was represented as a two-joint rigid linkage in a two-dimensional plane unaffected by gravity. The controller was a feed-forward desired torque profile modified by position and velocity feedback (proportional-derivative control). The model was constructed in Simulink and the control and analysis code was written in MATLAB.

The simulated arm was given the task of replicating free exploration movements produced by healthy control subjects. Healthy distributions were found to be similar to one another (mean R^2 = 0.81, 0.8, 0.9 for position, velocity and acceleration respectively), making them acceptable for use as the feed-forward driving signal for the simulation. The number of control subjects used in each simulation is addressed in the methods subsection dedicated to a description of library generation. These simulations result in a dense position trace that we separate into bins in a discrete distribution, or histogram, as seen on the right-hand side of Figure 1.

Movements were influenced by a combination of up to three idealized models of impairment (Figure 2, center bottom). Each of these models was based on a motor sign described in the clinical literature (Figure 3), although we make no claims as to the fidelity with which they replicate their namesakes. The goal was not to develop the best possible model to represent a set of motor signs but rather to develop a set of models that altered movement patterns in complex, nonlinear ways as motor impairments likely do in reality. All models had separate pathoparameters controlling the impairment at each joint, allowing a model to have, for instance, shoulder rigidity without elbow rigidity and vice versa. Rigidity was considered to be bi-directional, but the other two impairment models also distinguished between flexor and extensor impairments, resulting in four pathoparameters for each of them.

1) Rigidity

The first impairment we developed was a resisting torque, designed as a sigmoidal function of angular velocity about each joint. The parameters for this model were the maximal magnitudes of resisting torque at each joint. The equation for the sigmoid is as follows:

$$\tau_R = -\mathrm{R}\left(\frac{1-\mathrm{e}^{-\dot{\mathrm{q}}}}{1+\mathrm{e}^{-\dot{\mathrm{q}}}}\right)$$

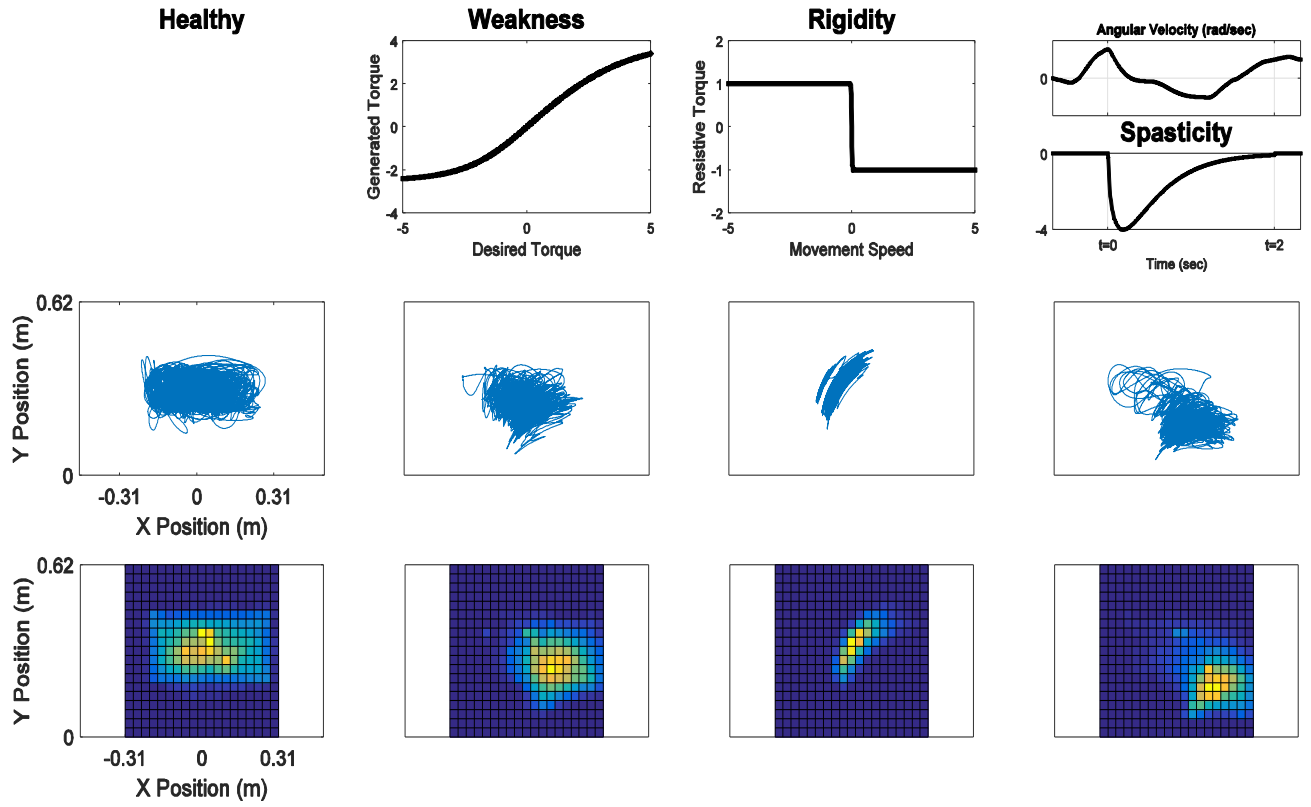

Figure 3. Impairment Model Examples. The first row displays the underlying motor impairment models responsible for the subsequent data. The second row displays position traces produced by simulations of movement with each of the above impairments. The third row displays distributions generated from the position traces in the second row.

where τ_R is the torque produced by the resistance model about a joint, R is the maximal magnitude of the resistance, and $\dot{q}$ is the angular velocity. There are thus two parameters governing this model, each of which represents the magnitude of resistance about a joint. This model is similar to clinical reports of rigidity, which describe it as either a steady or a ratcheting resistance to movement that is present irrespective of velocity(Terence D Sanger et al. 2010). Although it is typically viewed as a passive phenomenon, present only when the arm is manipulated by outside forces, it is possible that patients have simply learned the rigidity induced by their disease and compensate for it. Regardless, it serves as a useful test case of a nonlinear impairment.

2) Spasticity

For our second impairment, we developed a model based on clinical findings in patients with spasticity. This impairment model is a time-limited, "spasm" of torque triggered once angular velocity crosses a threshold value:

$$\tau_s = \begin{cases} -S_+ G(t), & \dot{q} > \dot{q_+} \\ 0, & \dot{q_-} < \dot{q} < \dot{q_+} \\ S_- G(t), & \dot{q} < \dot{q_-} \end{cases}$$

$$X(t) = C_m e^{-\frac{tC_t}{2}} \sqrt{tC_t + 10^{-3}}$$

where τ_s is the spasm torque, S is the maximal magnitude of the spasm, $\dot{q}$ is the angular velocity of the joint, $\dot{q_-}$ is the negative angular velocity trigger, $\dot{q_+}$ is the positive angular velocity trigger, "t" is time from start of the spasm and T is the duration of the spasm, chosen to be 2 seconds based on anecdotal clinician testimony. X(t) is a 3 degree of freedom Chi-Squared function, chosen because of its quick rise and slow die-off, which we believe captures the catch-and-release phenomenon described by clinicians when detecting spasticity(Braddom 2006; Francisco and McGuire 2008; Schmit et al. 1999). C_t and C_s are scaling constants derived from the Chi-Squared function; see Appendix for derivation. There were four parameters for this model; these represented the trigger velocity at each joint for clockwise and counterclockwise motions.

This spasm model is similar to clinical reports of spasticity or, "a motor disorder characterized by a velocity-dependent increase in tonic stretch reflexes (muscle tone) with exaggerated tendon jerks, resulting from hyper excitability of the stretch reflex"(Lance 1980). As with rigidity, we do not intend this model to be strictly accurate. Rather, it is a simplified stand-in for a more complex spasticity model such as might be used in the future.

3) Weakness

For our third impairment model, we developed a mathematical analogue for weakness. This model does not distinguish between neurological and physiological causes of weakness(Bohannon and Andrews 1998; Bourbonnais and Vanden Noven 1989). Rather, it acts at the level of torque output, attenuating the "desired" torque according to a piecewise sigmoidal function:

$$\tau_{actual} = W\left(\frac{1 - e^{C\tau_{desired}}}{1 + e^{C\tau_{desired}}}\right)$$

$$C = -\frac{2}{W}$$

where τ_{actual} is the torque produced about the joints, $\tau_{desired}$ is the desired torque and W is the saturation torque. This makes four parameters for this model: a maximum and a minimum torque about each joint. The value "C" has been chosen such that the maximum slope has been set to 1 at zero, thus making the function continuous (Appendix). This means that the simulation will be capable of accurately producing the desired torque at low values, but as the desired torque approaches saturation, the actual torque output will increasingly deviate from the desired. As mentioned before, this could either represent

a scenario in which the brain was unable to generate sufficient descending signal to the muscles or in which the muscles were themselves atrophied as a result of disuse. Either way, this represents a theoretically possible, nonlinear impairment in the torque domain.

B. Movement Distributions

We chose to use only the position data from the simulation rather than accept derivatives such as velocity and acceleration as outputs in our analysis because we felt this would best represent the kind of data we would receive from an actual robotic interface. We differentiated this position data to obtain velocity and acceleration. We also converted to angles using the manipulator Jacobian and then differentiated in order to obtain the first and second derivatives of angle. From this data, we generated six discrete two-dimensional movement distributions, or histograms: one set of position, velocity and acceleration each for Cartesian and angular space. Counts per bin were normalized to the total number of data points. Pathoparameter recovery was found to be similar across all six spaces, but best with angular acceleration (data not shown), so we chose to focus on angular acceleration as our distribution of choice. All data presented are acquired using angular acceleration distributions.

C. Parameter Estimation using Non-Negative Least Squares

In order to extract the model parameters from the endpoint position data, we used a non-negative least squares algorithm native to MATLAB. This optimization algorithm attempts to match an input vector by selecting from among the columns in a matrix. A vector of coefficients is generated that minimizes the residual between the input vector and the product of the coefficient vector with the matrix. The end result is a vector that weights a series of candidate vectors in such a way as to best match the input vector. In our case, the vector to be matched is a vectorized movement histogram, i.e. converted from an NxN histogram into a $1xN^2$ vector.

D. Library Generation

In order to test our hypothesis that models containing multiple motor impairments could be approximated by combinations of models containing individual impairments, we constructed a "library" of histograms generated by a variety of models of impairment. These histograms were vectorized to form the matrix that the non-negative least squares algorithm assigned coefficients to. These histograms, hereafter referred to as "library elements," were initially generated for single-impairment models only, i.e. models containing only weakness, only rigidity, or only spasticity. For comparison purposes, some pairwise combination models were later included as well. Initial observations of how impairment histograms deviated from healthy revealed an apparent exponential increase in the residuals as the impairment parameters approached 1 or 100%. We confirmed these observations by attempting recovery of a set of single-parameter models using a library that was linearly spaced and one

that was logarithmically spaced (data not shown). Because of this, we chose to space models equidistantly in log space according to the formula:

$$P_{log} = 1 - \log(9(1 - P_{lin}) + 1)$$

where P_{log} is the parameter in log space and P_{lin} is the parameter in linear space. This produces a series of values with log spacing while preserving the normalized 0 to 1 scale. For example, the first three elements in a series of ten "equally spaced" impairment models would be 22.9%, 41%, and 55.4% impaired.

For purposes of testing and illustration, we first constructed a library using only the two parameters related to shoulder extensor weakness and elbow rigidity. This impairment library contains 21 elements: ten for each of the two impairment parameters and one representing a "healthy" model. A visual representation of the pathoparameter estimation errors for our two-dimensional libraries can be seen in Figure 4. Because initial results had significant errors, we then tried two enhancements to the library: a model that contained 50% of each of the two impairments and a model that contained 100% of each of the two impairments. The goal was to maximize coverage of the impairment space by the library.

The main impairment library contains 101 elements: ten for each of the ten impairment parameters and one healthy. Because of the high dimensionality of this library, it became computationally infeasible to simulate all possible combinations of 50% impairments and 100% impairments as we did in the two-dimensional case. Instead, we included all pairwise combinations of 50% impairment and one model that was maximally impaired in all parameters. The reasoning behind this, as well as the conclusions we drew, are addressed in the discussion section.

Lastly, in order to test a more widely-distributed library, we also generated a 50-element Sobol set for both the two-dimensional case and the ten-dimensional case. A Sobol set is a quasi-random distribution of vectors of length N that covers the N-dimensional space more evenly than a random distribution does(Bratley and Fox 1988; Sobol' 1979). An example of this as applied to the two-dimensional case can be seen in the test models (red stars) displayed in Figure 4.

All libraries were constructed using simulations of four out of the five available healthy subjects' free exploration data. The movement histograms were therefore an average of the movement behaviors of all four healthy subjects. The test sets, which will be described in the next section, were constructed using the final subject only. The purpose behind this was to create a "training set" and a "test set," ensuring that the effects of the impairments on the histograms are detectable against between-subject variation.

E. Parameter Estimation Testing

In order to quantify the success in estimating a parameter set, we have chosen to use the Euclidean distance between the actual parameter vector and the estimated one, or the square root of the sum of the squares of the difference between the two vectors. We normalize this to the maximum possible distance between the two, which is the diagonal of an N-dimensional hypercube, where N is the number of active impairment parameters.

For the 2D case, we generated a 50 element test set in order to test the ability of the non-negative least squares algorithm to identify impairment parameters using each of the above libraries. For the ten-dimensional case we generated a 100 element test set due to concerns over the increase in dimensionality. These sets were both based on the Sobol Sequence, as described above. We also tested all libraries on the healthy distribution produced by the single subject used to generate all test data, to ensure that the variability between healthy controls was not large enough to overpower any differences we might see between distributions as a result of impairment models.

F. Statistics

Normality of the data was tested using the Anderson-Darling test. When data was non-normal, the correct distribution was estimated using the Kruskow-Wallis test. Significance of change in error between library types was tested using a one-way ANOVA, both without transformation and with the transformation recommended by the Kruskow-Wallis test. Because all libraries were used to identify the same set of test models, we also performed a series of paired t-tests with Bonferonni correction to test differences.

Chance levels of error were determined by replacing the non-negative least squares algorithm with a random number generator. This produced a vector of random values between zero and one for each test vector of pathoparameters. The difference between these two was considered to be the chance error.

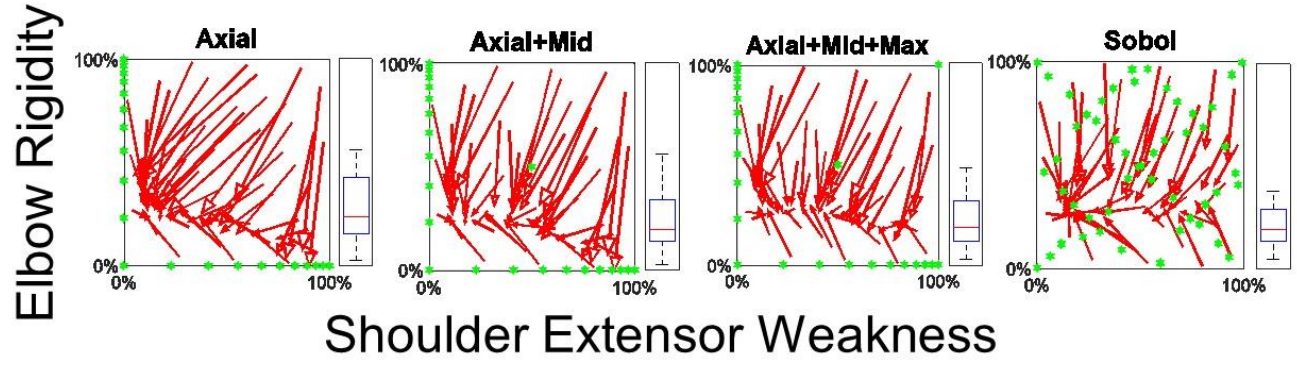

Figure 4. Error Plots for Two-Dimensional Example. Green stars represent library elements, red arrows represent error in pathoparameter space pointing from the true pathoparameter value to the estimated. Boxplots to the right of each error plot show the mean and quartiles of error normalized to maximum possible error ($\sqrt{2}$).

III. RESULTS

When attempting to identify the distributions produced by the healthy control "test" subject, we found pathoparameter errors for most library types. For the two-dimensional case, we found an error of 17.13% with the axial library and 18.54% with the Sobol distributed library. For the ten-dimensional case, we found an error of 7.95% with the axial library and 27.37% with the 51-element Sobol distributed library.

For the two-dimensional test problem, we found that there was a significant improvement from the basic axial library to all the other libraries and that there was borderline significance between the two enhanced axial libraries and the Sobol set library. See subsection F of the Methods section for details on the statistics used. The data for the two-dimensional case was found to be partially log-normal, so all statistics were run on both the raw data set and on the data after a log transform. Using ANOVA, there was no significant difference between groups with the log transform ($p = 0.26$). A multiple comparisons test on the groups without the transform revealed a significant difference between the axial and Sobol set libraries ($P = 0.0496$). Paired t-tests revealed a significant difference between the axial and all other conditions and between the axial+mid and all others, but not for any other model pairings and produced the same results both before and after the log transform. All four library structures

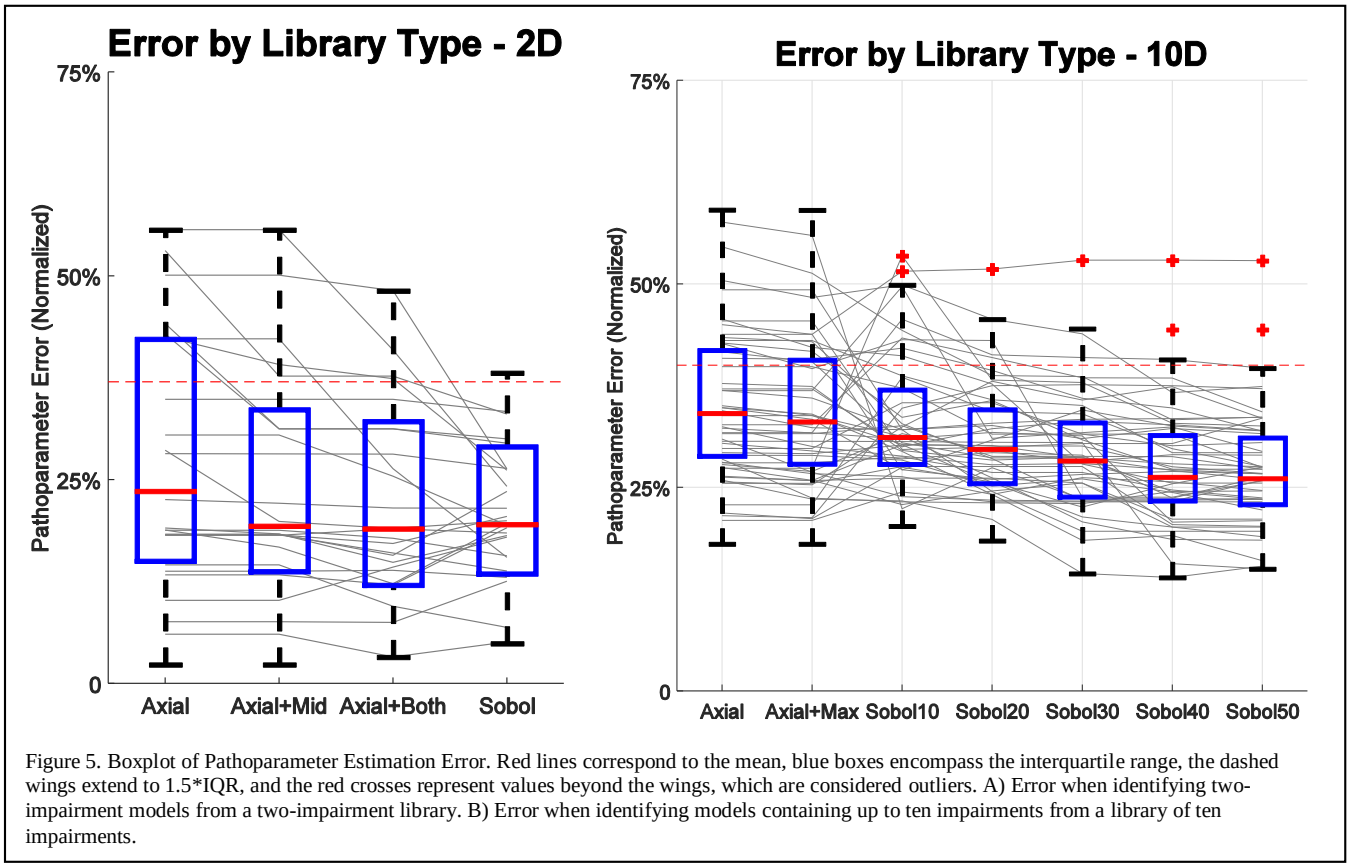

Figure 5. Boxplot of Pathoparameter Estimation Error. Red lines correspond to the mean, blue boxes encompass the interquartile range, the dashed wings extend to 1.5*IQR, and the red crosses represent values beyond the wings, which are considered outliers. A) Error when identifying two-impairment models from a two-impairment library. B) Error when identifying models containing up to ten impairments from a library of ten impairments.

performed better than chance, which was determined to be 37%. See subsection F of the Methods section for details on how this was determined. We found an average parameter estimation error of 26.8% across unknown models when performing identification using an axial library, 23.9% using an axial library plus a halfway impaired model, and 21.9% using an axial library with both a halfway and a fully impaired model. The error using a Sobol set as a library averaged 20.4%.

In the ten-dimensional case, we found that there was no significant difference between the two axial library types and the 11-element Sobol set. Both of the axial libraries performed significantly worse than the other four Sobol set libraries. No significance was found between any adjacent Sobol set libraries, i.e. those with 10 more or fewer elements than one another. Paired t-tests found significant differences between all pairs of libraries except for between the 11-element Sobol set library and the two axial libraries. Both axial library layouts performed at levels worse than chance (40%). Performance was only improved beyond chance when a Sobol distributed library was used. We found an average parameter estimation error of 35.3% (normalized Cartesian distance) when identifying models in a Sobol set using an axial library, and 34.3% for an axial library plus a model with maximal levels of all ten impairments. For Sobol set libraries containing 11, 21, 31, 41, and 51 models, the average errors were 32.6%, 30.3%, 28.7%, 27.5%, and 26.8%, respectively. See Figure 5.

We also tested the similarity between distributions of impaired movements as an analogy to the cost surface (Figure 6). For the ten-dimensional case, R^2 between distributions rarely exceeded 0.8, indicating a high likelihood that there is a unique mapping from distributions to pathoparameter sets. Figure 6B also reveals some systematic patterns of similarity between distributions representative of different types of impairment. The first pattern is a series of dark regions associated with the main diagonal in columns associated with impairments in extensors. Another pattern of similarity can be seen in the columns corresponding to flexor impairments, where diagonal lines appear almost parallel to the main axis. There is a similar diagonal line in boxes that compare flexor impairment with shoulder rigidity. Finally, there are some dark lines that appear to have a slope opposite the main diagonal in boxes corresponding to comparisons between elbow flexor spasticity and elbow rigidity and between elbow flexor spasticity and shoulder extensor spasticity. See the discussion for an interpretation of these patterns.

A

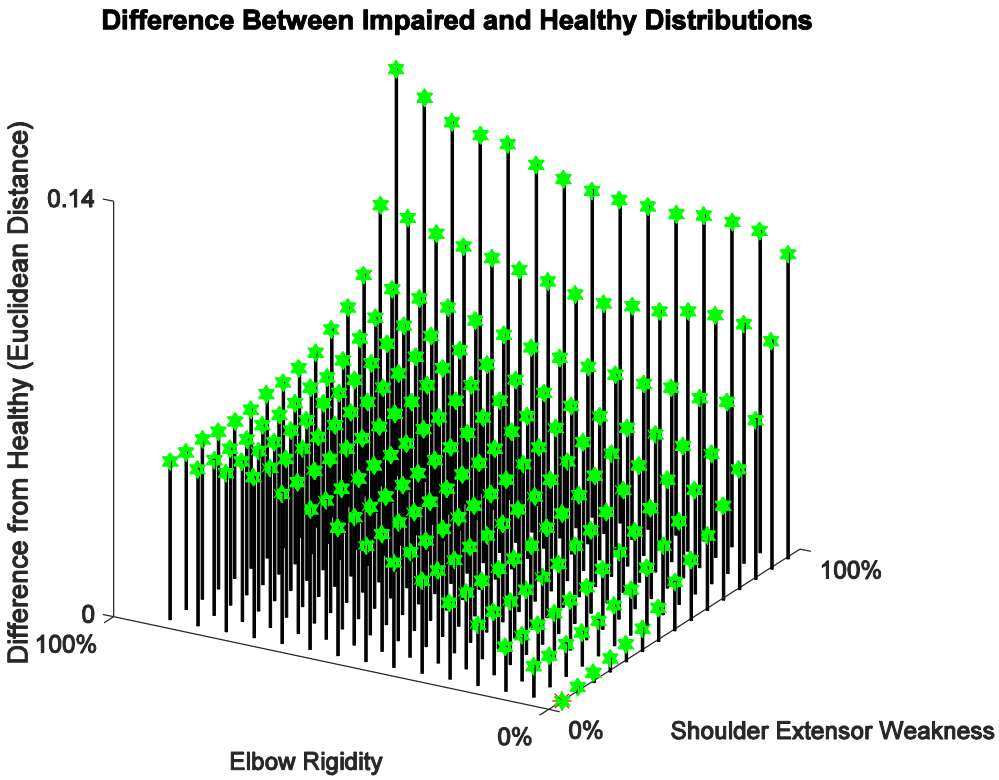

B

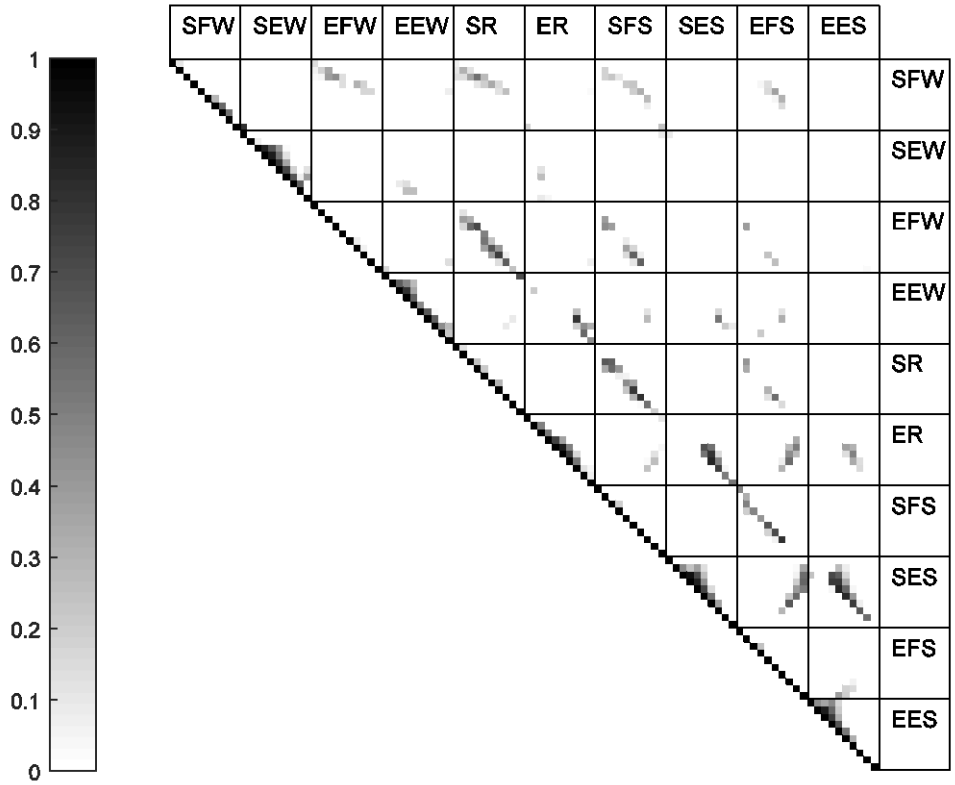

Figure 6. Difference of Distributions from Healthy. A) A plot of Euclidean distance (square root of the sum of the squares) between a healthy distribution and a set of impaired distributions as a function of degree of impairment in shoulder extensor weakness and elbow rigidity. The two-dimensional model allows a view of the full "cost surface" between axes. B) A plot of the 10-D case, showing the R^2 (coefficient of determination) between distributions for various values of all ten pathoparameters. High R^2 indicates a high degree of similarity between distributions.

IV. DISCUSSION

This study used a synthetic model of human free exploration and an impairment modeling framework to investigate the feasibility of using distributions of movement probabilities to identify the sources of motor pathology. We found that there is a smooth and continuous relationship in the mapping between the parameters governing idealized pathologies (pathoparameters) and the distributions that they give rise to. We found that increased care is warranted when mixed sets of pathologies are present in a single model in order to avoid confusion between similar distributions. This technique, although imperfect, gives new hope for the use of movement probability distributions as a new tool for understanding the functional behavior of motor deficits and their interactions with one another and with the task environment.

Despite being generated from a healthy subject, the "control" distribution was misdiagnosed by the axial and the Sobol distributed libraries for both the two-dimensional and the ten-dimensional case. This indicates that the variability between healthy free-exploration controls is large enough to be of concern when attempting to identify the pathoparameters responsible for each generated distribution. It is worth keeping the size of the error identifying healthy distributions into account when considering the errors obtained when trying to identify impaired distributions as a point of reference. If the errors are comparable, then it is not possible to determine whether they are attributable to our system identification methods or to the inherent variability between subjects, which means that they should not be taken as an indictment of our lookup-table approach.

In both the two-dimensional and the ten-dimensional case, the simple axial library performed significantly worse than the Sobol distributed library at identifying the underlying pathoparameters responsible for the observed distributions. This appears to be a strong refutation of the hypothesis that motor impairments can be combined in a linear manner. It is a common belief in the field of human motor control research that movements are controlled via a group of low-level muscle synergies that are shifted and scaled in time and magnitude to produce the repertoire of behaviors displayed in daily life(d'Avella, Saltiel, and Bizzi 2003; Latash, Scholz, and Schöner 2007). If this were the case, one might expect that motor impairments, which would be characterized by damaged or altered synergies(Terence D Sanger et al. 2006), might be similarly recombinable. However, a recent paper by Steele, Tresch and Perreault suggests that the biomechanical constraints of the human body and of the tasks that subjects are performing may make it very difficult to identify synergies using matrix factorization techniques(Steele, Tresch, and Perreault 2015). Since non-negative least squares is a sub-problem of non-negative matrix factorization(Kim and Park 2008; Lin 2007), it is therefore not a surprise that our own task, which is constrained to planar motion, yields results with some level of confusion and ambiguity.

Although there was an increase in performance between the 11-element Sobol distributed library in the ten-dimensional case and the 51-element library, the improvement was relatively minor, with only a 5.8% drop in error. One possible interpretation is that interpolation within pathoparameter space based on distributions is infeasible; we believe that it is more likely that this phenomenon is caused by the "curse of dimensionality"(Stix 2015). In brief, as the dimensionality of a space increases linearly, its size increases. Some of the consequences of this include a reduction in normalized distance between points(François, Wertz, and Verieysen 2007) and an exponential increase in the number of points needed to adequately characterize or span the space(Kuo and Sloan 2005; Chávez et al. 2001). Because we are comparing 20x20 distributions, or 400-element vectors, we find ourselves attempting to map relationships in a 400-dimensional distribution space to ones in an $N \leq 10$ dimensional space, the pathoparameter space. This causes problems that get gradually worse as N increases.

For instance, consider the case where $N = 1$. In this situation, we are changing a single pathoparameter and observing a change between a healthy and maximally impaired distribution. Assuming a mostly smooth mapping, this will result in a curve passing through 400-dimensional distribution space. Points on the pathoparameter line will map to points on the distribution space curve and identification should be fairly trivial provided there are several evenly-spaced library elements along the line. Now consider the case where $N = 2$. In this case, we are mapping from a bounded plane in pathoparameter space (Figure 6A) to a surface in 400-dimensional distribution space bounded by the vertices corresponding to healthy, maximally impaired in each pathoparameter and maximally impaired in both pathoparameters. The surface area of this surface in distribution space, however, may be far larger than the surface area of the pathoparameter space plane because of the enormously increased size of 400-dimensional space. As a result, sparseness begins to become a problem, so that while library elements may be distributed evenly in pathoparameter space, they may be very dense in certain regions of distribution space and very sparse in others.

Our rescaling of the axial library to be log-distributed was a simple attempt to alleviate this problem, but the axial library's poor performance in the two-dimensional case, much less the ten-dimensional scenario, shows that a more comprehensive approach is needed. Using a Sobol set, which was developed with searches in high-dimensional parameter space in mind, was the next step up in complexity, and it yielded significant improvements. It would, however, be prohibitively costly to attempt to blindly add more models from the Sobol sequence to keep improving results because the number of models needed to bring the accuracy up will be enormous in even a ten-dimensional pathoparameter space. This is clearly demonstrated by the fact that going from an 11-element to a 51-element Sobol distributed library in the ten-dimensional case only resulted in a 5.8% reduction of error, although this is only approximately 5% away from the performance of the two-dimensional Sobol distributed library.

In Figure 4, there are clear regions, roughly linear in shape, which appear to "attract" the non-negative least squares algorithm. This is an example of "hubness," or the tendency for certain models to be chosen excessively frequently by metric matching

algorithms such as K nearest neighbors. We believe that this is the cause of the poorer accuracy in the ten-dimensional case. Hubness arises as a result of certain models being closer to the mean than most, a situation that high dimensionality exacerbates by compressing the space of the actual data points(Nanopoulos 2010). As the dimensionality of the pathoparameter space increases, this tendency for certain elements on the axes to pull the non-negative least squares algorithm away from the extrema will only worsen the quality of pathoparameter estimation. Although the two-dimensional Sobol set appears to have some hubs in it as well (Figure 4, far right), this appears to have less of an impact on the estimation error. This is likely because the Sobol set contains elements that are near the interior of the space, which are a better guess on average than points at the edges because they are more likely to be close to any random point in the space. Fortunately, there are ways to resolve this problem, some of which turn hubness to their advantage to make faster, more accurate searches of the space(Tomašev et al. 2011).

In order to better understand the mapping between pathoparameter space and distribution space, we also visualized the relationship between pathoparameter values and change in the distributions. It was our hope that this would help us identify distinct regions in pathoparameter space that corresponded to a single region of distribution space, allowing us to locate potential regions of confusion. Figure 6A gives us a visual of the magnitude of change in distribution space relative to healthy as a function of pathoparameter position. Although this scalar measure of difference is a collapsed, one-dimensional representation of a complex, high-dimensional space, we know that arithmetic functions performed on one smooth surface will result in another(J. Lee 2012), so it is reasonable to regard this as supporting our belief that the 400-dimensional surface in distribution space is also smooth. Two more observations are also worth noting. The first is that the rate of change is very different for the two pathoparameter directions, meaning that we now have quantitative evidence that some impairment models will have a greater impact on the resultant distribution than others. The second is that there is a region of relative flatness out in the region near [0.25, 1], which is indicative of an area of low rates of change. Attempts to identify pathoparameter values that fall within this sort of region will be very vulnerable to noise and hubness.

Figure 6B, the correlation matrix between all single-impairment movement distributions, offers a more comprehensive look at the relationship between pathoparameter values and distribution shapes. Here we can see regions of high similarity, analogous to the flat region of 6A, as dark patches. The darker the patch, the higher the coefficient of determination between the distributions being compared, which can be taken as a measure of how close the distributions are to one another in distribution space. From this matrix, we draw several conclusions: that flexor impairments are easier to observe than extensor impairments; that impairments with very different underlying models can produce very similar behaviors; and that flexor and extensor impairments are anti-correlated.

The dark regions along the main diagonal all fall into columns corresponding to extensor impairments. This indicates models that are close to one another on extensor pathoparameter axes have a high degree of similarity. This, in turn, suggests that altering the activity of the extensors has a relatively small impact on the shape of the distribution. If the impact were large, then changing the pathoparameter by even a small amount would result in a new distribution that had a very low correlation coefficient with the previous one. The relative lack of impact is likely because our upper extremity flexors are generally stronger than our extensors so we are more likely to use them to make strong or fast motions(Amis, Dowson, and Wright 1979).

This is supported by the existence of the secondary diagonal, which mostly shows that flexor impairments and extensor impairments follow a similar path through distribution space as they increase. In other words, the movement distribution evolves similarly whether you're increasing flexor weakness or flexor spasticity. The same phenomenon occurs for extensor impairments, but the effect is weaker. This discovery is something of a mixed blessing. On the one hand, it means that we don't have to worry about movement distributions falling into too large a region of their 400-dimensional space because motor impairments, likely because of kinematic constraints, tend to follow similar paths in that space. On the other hand, this means that there is potential for confusion between very different impairments. We therefore need to identify the regions of distribution space in which different impairments become close to one another and check to ensure that the distribution-impairment surfaces do not touch or cross. If they do, that means that those impairments are indistinguishable from one another at that point.

It is also interesting to note the difference between shoulder and elbow rigidity. We hypothesize that shoulder rigidity has more of an impact on movement distributions than elbow rigidity because movements from the shoulder can be used to help move the elbow via Coriolis and centripetal forces, while elbow movements have very little influence on motion at the shoulder joint. This would explain why shoulder rigidity produces similar distributions to flexor impairments, which we have established as more noticeable than extensor impairments; both are responsible for large limitations in the ability of the arm to move. Elbow rigidity, on the other hand, seems to be correlated with extensor spasticity, which is responsible for smaller changes to the distribution. Most interesting of all is the fact that elbow rigidity appears anti-correlated with flexor spasticity. This would indicate that the paths these impairments follow through distribution space are reversible in a way that the paths for weakness-based impairments are not. Or, put another way, it should be possible to predict extensor spasticity distributions using flexor spasticity distributions and vice-versa, at least for moderate levels of impairment that do not fall at either the high or the low end of the pathoparameter spectrum.

In conclusion, we have developed and tested a lookup table-based approach to recovering the pathoparameter associated with impaired movement distributions produced by a dynamic simulation of a free exploration task. This process has revealed a number of important considerations for attempts to perform system identification on individuals with complex combinations of

impairments present. Despite the fact that the curse of dimensionality is typically cited as a problem in data sets with dimensionality many orders of magnitude higher than those associated with this study, we still found that it still negatively impacted our non-negative least squares algorithm's performance. Future efforts towards the goal of pathoparameter recovery from distributions will likely need to make full use of the tools developed to combat this problem, such as lattice rule construction algorithms(Kuo and Sloan 2005) and support vector machines(Alonso, Malpica, and de Agirre 2011). This process has also, however, revealed that the hypervolume in distribution space occupied by possible models of impairment is of manageable size while still preserving spacing between distributions. This means that the task of uniquely identifying the pathoparameters associated with given distributions remains feasible.

Although this study exhibits a number of limitations in its approach and simplicity, it is important to note that this was an exploratory effort. Our goal was not to comprehensively define and identify motor impairment models in stroke survivors; our models are, in fact, very rudimentary and only cover the most basic aspects of their namesakes. Rather, it was our intent to explore the evolution of motor behavior, as captured by distributions, in response to changing types and levels of impairment and to determine if those distributions could be used to uniquely determine the underlying pathoparameters controlling the impairment models. And in this, we feel that we have succeeded by verifying the feasibility of pathoparameter identification using movement distributions.

Nevertheless, it is worth discussing the limitations of the study to put our results in context and to identify the most important steps to take next. First is the decision to use simulations rather than patient data for our study. Because of the complex nature of impairments in stroke survivors, and because impairments in this population are almost never isolated, we felt that it was necessary to perform this research in the context of a simulation rather than actual stroke subject data. In this way, we were able to keep track of all the parameters and observe data flow from one element of our simulation to another, which let us focus on the basic question of whether or not pathoparameter recovery was feasible. It could have been the case that the loss of time and frequency information inherent to the use of static distributions would have rendered such recovery impossible. Or it could have been that different impairment models produce identical distributions, rendering them structurally non-identifiable(Chis, Banga, and Balsa-Canto 2011). Performing this study *in silico* allowed us to rule out such possibilities before investing the time and resources to develop a human subjects research protocol.

Another potential point of concern is our choice of driving signal. By using healthy free exploration as a driving signal for our simulations, we are assuming that stroke survivors would plan to move as healthy individuals do. This has been called into question for constrained tasks such as straight-line reaching(Mccrea et al. 2005; Roby-Brami et al. 2003), so it is certainly an important question to consider. The purpose of free exploration, however, is to try to obtain information about a subject's

movement tendencies. All subjects perform a different sequence of motions under these conditions, but healthy distributions have been found to be highly correlated with one another (see Methods A), which suggests that there is a kind of universal drive independent of the individual sub-movements that make up a free exploration trial. It might be worthwhile to test this hypothesis in the future by using a driving signal constructed using randomized torque inputs designed to have the same frequency and power content of healthy human movement, but we believe that our current method adequately captures the basics of the effects of motor impairments upon movement.

We made the choice of focusing exclusively on angular acceleration rather than on the other five spaces based on preliminary tests in which variability in performance between test models was very high relative to variability between the six spaces, but angular acceleration seemed to produce more consistent results than the others. We regard this as unsurprising, since the behavior of the simulation was manipulated at the torque level, and torque is a function of angular acceleration and the physical properties of the system. Another alternative to using one of the six aforementioned spaces would be using them in combination, i.e. having an N-dimensional discrete distribution instead of merely 3-dimensional (X, Y and count). While this may have increased the specificity of our identification, it would also have made the distribution space even more high-dimensional and thus run the risk of creating extreme sparseness. This concern, combined with the number of possible combinations that would have had to have been tested, chose us to skip this analysis. It does, however, remain a viable possibility for future work.

For this work, we chose to weight all bins within the discrete distributions equally. There are, however, different methods of selecting basis functions offered from the data (such as eigenvalue decomposition) and of pre-conditioning the data (such as PCA) that might improve our pathoparameter recovery. Such alternative methods are linear manipulations, yet may still be informative and useful. However, we must consider that this would require simulations corresponding to a large number of points within the ten-dimensional pathoparameter space, and hence may be computationally infeasible. It might also be possible to perform a similar dimension reduction process, or a method specifically designed to choose bases that are as close to orthogonal as possible, to identify which combinations of impairments are most readily separable from one another. It remains to be seen if such linear preconditioning of data might help to improve outcomes.

The most potentially controversial aspect of this work is almost certainly our choice of impairment models. We chose to create simple, torque-based models of impairments rather than using the complex body of research that has been done on patients with symptoms such as spasticity and weakness for the same reason we chose to use simulations instead of studying stroke survivors: simplicity and the ability to observe and understand the flow of data in the model. In the design of our models, we consciously chose to ensure that the functions that generated them were smooth and made use of mathematical structures that are commonly seen in nature, such as the Gaussian distribution and sigmoid functions(Bejan and Lorente 2011). We believe that

this preserves the basic physical character of these impairments and lends enough realism to our results for this preliminary investigation. Most importantly, we have constructed a framework into which any model of impairment can be easily inserted, allowing for more detailed exploration of different types of impairments and perhaps even comparisons or competitions between different models of the same impairments.

In recent years, we have begun to see some efforts made towards modeling and identification of impairments in individual patients. These have generally been oriented towards quantification of severity and restricted to single impairments in single joints or isometric tasks(Mirbagheri et al. 2001; Alibiglou et al. 2008; Meskers et al. 2009). In this study, we have developed a high-level, model-based system for identifying and quantifying motor impairments in the upper extremity using movement distributions. We have successfully identified the underlying pathoparameters of these motor impairments at almost 25% accuracy for a ten-dimensional test sample and in so doing have revealed both obstacles and opportunities for improvement. Most importantly, we have confirmed the feasibility of such an identification procedure. This work represents a first step towards improved characterization of motor impairments in survivors of stroke and other neurological trauma, which will enhance our ability to study and treat these symptoms.

REFERENCES

Alibiglou, Laila, William Z Rymer, Richard L Harvey, and Mehdi M Mirbagheri. 2008. "The Relation between Ashworth Scores and Neuromechanical Measurements of Spasticity Following Stroke." *Journal of Neuroengineering and Rehabilitation* 5 (January): 18. doi:10.1186/1743-0003-5-18.

Alonso, María C, José A Malpica, and Alex Martínez de Agirre. 2011. "Consequences of the Hughes Phenomenon on Some Classification Techniques." In *ASPRS 2011 Annual Conference*. Milwaukee, Wisconsin.

Amis, A A, D Dowson, and V Wright. 1979. "Muscle Strengths and Musculoskeletal Geometry of the Upper Limb." *Engineering in Medicine* 8 (1): 41–48. doi:10.1243/EMED_JOUR_1979_008_010_02.

Bejan, a., and S. Lorente. 2011. "The Constructal Law Origin of the Logistics S Curve." *Journal of Applied Physics* 110 (2): 024901. doi:10.1063/1.3606555.

Bohannon, R W, and A W Andrews. 1998. "Relationships between Impairments in Strength of Limb Muscle Actions Following Stroke." *Percept Mot Skills* 87 (3 Pt 2): 1327–30. http://www.ncbi.nlm.nih.gov/pubmed/10052093.

Bourbonnais, Daniel, and S Vanden Noven. 1989. "Weakness in Patients with Hemiparesis." *The American Journal of Occupational Therapy : Official Publication of the American Occupational Therapy Association* 43 (5): 313–19. doi:10.5014/ajot.43.5.313.

Braddom, Randall L. 2006. "Physical Medicine and Rehabilitation." In , edited by Ralph M. Buschbacher, Leighton Chan, Karen J. Kowalske, Edward R. Laskowski, Dennis J. Matthews, Kristen T. Richardson, and Richard W. Johnson, 3rd ed., 1504. Elsevier.

Bratley, Paul, and Bennett L. Fox. 1988. "ALGORITHM 659: Implementing Sobol's Quasirandom Sequence Generator." *ACM Transactions on Mathematical Software* 14 (1): 88–100. doi:10.1145/42288.214372.

Chávez, Edgar, Gonzalo Navarro, Ricardo Baeza-Yates, and José Luis Marroquín. 2001. "Searching in Metric Spaces." *ACM Computing Surveys* 33 (3): 273–321. doi:10.1145/502807.502808.

Chen, Donghui, and Robert J Plemmons. 2009. "Nonnegativity Constraints in Numerical Analysis." *Proceedings of Symposium on the Birth of Numerical Analysis*, 1–32. doi:10.1142/9789812836267_0008.

Chis, Oana-Teodora, Julio R Banga, and Eva Balsa-Canto. 2011. "Structural Identifiability of Systems Biology Models: A Critical Comparison of Methods." *PloS One* 6 (11): e27755. doi:10.1371/journal.pone.0027755.

Cramer, Steven C, Walter J Koroshetz, and Seth P Finklestein. 2007. "The Case for Modality-Specific Outcome Measures in Clinical Trials of Stroke Recovery-Promoting Agents." *Stroke; a Journal of Cerebral Circulation* 38 (4): 1393–95. doi:10.1161/01.STR.0000260087.67462.80.

d'Avella, Andrea, Philippe Saltiel, and Emilio Bizzi. 2003. "Combinations of Muscle Synergies in the Construction of a Natural Motor Behavior." *Nature Neuroscience* 6 (3): 300–308. doi:10.1038/nn1010.

Flash, T, and N Hogan. 1985. "The Coordination of Arm Movements: An Experimentally Confirmed Mathematical Model." *The Journal of Neuroscience* 5 (7): 1688–1703. http://www.jneurosci.org/content/5/7/1688.short.

Francisco, Gerard E, and John R McGuire. 2008. "Stroke Recovery and Rehabilitation." In , edited by Joel Stein, Richard L Harvey, Richard F Macko, Carolee J Winstein, and Richard D Zorowitz, 1st ed., 992. Demos Medical.

François, Damien, Vincent Wertz, and Michel Verleysen. 2007. "The Concentration of Fractional Distances." *IEEE Transactions on Knowledge and Data Engineering* 19 (7): 873–86. doi:10.1109/TKDE.2007.1037.

Gladstone, D. J., S. E. Black, and a. M. Hakim. 2002. "Toward Wisdom From Failure: Lessons From Neuroprotective Stroke Trials and New Therapeutic Directions." *Stroke* 33 (8): 2123–36. doi:10.1161/01.STR.0000025518.34157.51.

Gladstone, David J, Cynthia J Danells, and Sandra E Black. 2002. "The Fugl-Meyer Assessment of Motor Recovery after Stroke: A Critical Review of Its Measurement Properties." *Neurorehabilitation and Neural Repair* 16 (3): 232–40. doi:10.1177/154596802401105171.

Huang, Felix C, and James L Patton. 2013. "Individual Patterns of Motor Deficits Evident in Movement Distribution Analysis." *IEEE ... International Conference on Rehabilitation Robotics : [proceedings]* 2013: 1–6. doi:10.1109/ICORR.2013.6650430.

Huang, Vincent S, and John W Krakauer. 2009. "Robotic Neurorehabilitation: A Computational Motor Learning Perspective." *Journal of Neuroengineering and Rehabilitation* 6 (January): 5. doi:10.1186/1743-0003-6-5.

Ivanhoe, Cindy B., and Timothy a. Reistetter. 2004. "Spasticity." *American Journal of Physical Medicine & Rehabilitation* 83 (Supplement): S3–9. doi:10.1097/01.PHM.0000141125.28611.3E.

Kim, Hyunsoo, and Haesun Park. 2008. "Nonnegative Matrix Factorization Based on Alternating Nonnegativity Constrained Least Squares and Active Set Method." *SIAM Journal on Matrix Analysis and Applications* 30 (2): 713–30. doi:10.1137/07069239X.

Kuo, Frances Y, and Ian H Sloan. 2005. "Lifting the Curse of Dimensionality." *Notices of the AMS* 52 (11): 1320–28.

Kwakkel, Gert, Boudewijn J Kollen, and Hermano I Krebs. 2008. “Effects of Robot-Assisted Therapy on Upper Limb Recovery after Stroke: A Systematic Review.” *Neurorehabilitation and Neural Repair* 22 (2): 111–21. doi:10.1177/1545968307305457.

Lackner, James R, and Paul Dizio. 2009. “Control and Calibration of Multi-Segment Reaching Movements.” Edited by Dagmar Sternad, Advances in Experimental Medicine and Biology, 629. Boston, MA: Springer US. doi:10.1007/978-0-387-77064-2.

Lance, J W. 1980. “The Control of Muscle Tone, Reflexes, and Movement: Robert Wartenberg Lecture.” *Neurology*, no. 30: 113–30.

Latash, Mark L, John P Scholz, and Gregor Schöner. 2007. “Toward a New Theory of Motor Synergies.” *Motor Control* 11 (3): 276–308. http://www.ncbi.nlm.nih.gov/pubmed/17715460.

Latash, Mark L. 2010. “Motor Control: In Search of Physics of the Living Systems.” *Journal of Human Kinetics* 24 (-1): 7–18. doi:10.2478/v10078-010-0015-4.

Le Cavorzin, Philippe, S. Annick Poudens, Francis Chagneau, Guy Carrault, Herv Allain, and Pierre Rochcongar. 2001. “A Comprehensive Model of Spastic Hypertonia Derived from the Pendulum Test of the Leg.” *Muscle and Nerve* 24 (12): 1612–21. doi:10.1002/mus.1196.

Lee, D O Q. 2012. “Numerically Efficient Methods for Solving Least Squares Problems,” 1–15.

Lee, JohnM. 2012. “Smooth Maps.” In *Introduction to Smooth Manifolds SE - 2*, 218:32–49. Graduate Texts in Mathematics. Springer New York. doi:10.1007/978-1-4419-9982-5_2.

Lin, Chih-Jen. 2007. “Projected Gradient Methods for Nonnegative Matrix Factorization.” *Neural Computation* 19 (10): 2756–79. doi:10.1162/neco.2007.19.10.2756.

Mccrea, Patrick H, Janice J Eng, Antony J Hodgson, H Patrick, Janice J Eng, and Antony J Hodgson. 2005. “Saturated Muscle Activation Contributes to Compensatory Reaching Strategies After Stroke,” 2999–3008. doi:10.1152/jn.00732.2004.

Meskers, Carel G M, Alfred C Schouten, Jurriaan H de Groot, Erwin de Vlugt, Bob J J van Hilten, Frans C T van der Helm, and Hans J H Arendzen. 2009. “Muscle Weakness and Lack of Reflex Gain Adaptation Predominate during Post-Stroke Posture Control of the Wrist.” *Journal of Neuroengineering and Rehabilitation* 6 (January): 29. doi:10.1186/1743-0003-6-29.

Mirbagheri, M M, H Barbeau, M Ladouceur, and R E Kearney. 2001. “Intrinsic and Reflex Stiffness in Normal and Spastic, Spinal Cord Injured Subjects.” *Experimental Brain Research* 141 (4): 446–59. doi:10.1007/s00221-001-0901-z.

Mostafavi, Sayyed Mostafa, Janice I Glasgow, Sean P Dukelow, Stephen H Scott, and Parvin Mousavi. 2013. “Prediction of Stroke-Related Diagnostic and Prognostic Measures Using Robot-Based Evaluation.” *IEEE ... International Conference on Rehabilitation Robotics : [proceedings]* 2013: 6650457. doi:10.1109/ICORR.2013.6650457.

Nanopoulos, Alexandros. 2010. “Hubs in Space : Popular Nearest Neighbors in High-Dimensional Data.” *Journal of Machine Learning Research* 11: 2487–2531. http://jmlr.csail.mit.edu/papers/volume11/radovanovic10a/radovanovic10a.pdf.

Prange, Gerdienke B., Michiel J. a. Jannink, Catharina G. M. Groothuis-Oudshoorn, Hermie J. Hermens, and Maarten J. IJzerman. 2006. “Systematic Review of the Effect of Robot-Aided Therapy on Recovery of the Hemiparetic Arm after Stroke.” *The Journal of Rehabilitation Research and Development* 43 (2): 171. doi:10.1682/JRRD.2005.04.0076.

Reinkensmeyer, David J., Jeremy L. Emken, and Steven C. Cramer. 2004. “Robotics, Motor Learning, and Neurologic Recovery.” *Annual Review of Biomedical Engineering* 6 (1): 497–525. doi:10.1146/annurev.bioeng.6.040803.140223.

Reuben, David B, Susan Magasi, Heather E McCreath, Richard W Bohannon, Ying-Chih Wang, Deborah J Bubela, William Z Rymer, et al. 2013. “Motor Assessment Using the NIH Toolbox.” *Neurology* 80 (11 Supplement 3): S65–75. doi:10.1212/WNL.0b013e3182872e01.

Roby-Brami, a, a Feydy, M Combeaud, E V Biryukova, B Bussel, and M F Levin. 2003. “Motor Compensation and Recovery for Reaching in Stroke Patients.” *Acta Neurologica Scandinavica* 107 (5): 369–81. doi:021 [pii].

Sanger, T. D., M. R. Delgado, D. Gaebler-Spira, M. Hallett, and J. W. Mink. 2003. “Classification and Definition of Disorders Causing Hypertonia in Childhood.” *Pediatrics* 111 (1): e89–97. doi:10.1542/peds.111.1.e89.

Sanger, Terence D, Daofen Chen, Mauricio R Delgado, Deborah Gaebler-Spira, Mark Hallett, and Jonathan W Mink. 2006. “Definition and Classification of Negative Motor Signs in Childhood.” *Pediatrics* 118 (5): 2159–67. doi:10.1542/peds.2005-3016.

Sanger, Terence D, Daofen Chen, Darcy L Fehlings, Mark Hallett, Anthony E Lang, Jonathan W Mink, Harvey S Singer, et al. 2010. “Definition and Classification of Hyperkinetic Movements in Childhood.” *Movement Disorders : Official Journal of the Movement Disorder Society* 25 (11): 1538–49. doi:10.1002/mds.23088.

Sarbaz, Yashar, Shahriar Gharibzadeh, Farzad Towhidkhah, Masood Banaie, and Ayyoob Jafari. 2011. “A Gray-Box Neural Network Model of Parkinson’s Disease Using Gait Signal.” *Basic and Clinical ...* 2 (3): 33–42. http://bcn.iums.ac.ir/browse.php?a_code=A-10-1-59&slc_lang=fa&sid=1.

Schmit, B D, Y Dhaher, J P Dewald, and W Z Rymer. 1999. “Reflex Torque Response to Movement of the Spastic Elbow: Theoretical Analyses and Implications for Quantification of Spasticity.” *Annals of Biomedical Engineering* 27 (6): 815–29. http://www.ncbi.nlm.nih.gov/pubmed/10625153.

Scott, Stephen H., and Sean P. Dukelow. 2011. “Potential of Robots as next-Generation Technology for Clinical Assessment of Neurological Disorders and Upper-Limb Therapy.” *The Journal of Rehabilitation Research and Development* 48 (4): 335. doi:10.1682/JRRD.2010.04.0057.

Shadmehr, R, and FA Mussa-Ivaldi. 1994. “Adaptive Representation of Dynamics during Learning of a Motor Task.” *The Journal of Neuroscience* 74 (May). http://www.jneurosci.org/content/14/5/3208.short.

Sobol’, I. M. 1979. “On the Systematic Search in a Hypercube.” *SIAM Journal on Numerical Analysis* 16 (5): 790–93. doi:10.1137/0716058.

Steele, Katherine M., Matthew C. Tresch, and Eric J. Perreault. 2015. “Consequences of Biomechanically Constrained Tasks in the Design and Interpretation of Synergy Analyses.” *Journal of Neurophysiology* 113 (7): 2102–13. doi:10.1152/jn.00769.2013.

Stix, Gary. 2015. “Lifting the Curse of Alzheimer’s.” *Scientific American* 312 (5): 50–57. doi:10.1038/scientificamerican0515-50.

Tomašev, Nenad, Miloš Radovanović, Dunja Mladenić, and Mirjana Ivanović. 2011. “The Role of Hubness in Clustering High-Dimensional Data.” *Lecture Notes in Computer Science (including Subseries Lecture Notes in Artificial Intelligence and Lecture Notes in Bioinformatics)* 6634 LNAI (PART 1): 183–95. doi:10.1007/978-3-642-20841-6-16.

Tsuji, T, M Liu, S Sonoda, K Domen, and N Chino. 2000. “The Stroke Impairment Assessment Set: Its Internal Consistency and Predictive Validity.” *Archives of Physical Medicine and Rehabilitation* 81 (7): 863–68. doi:10.1053/apmr.2000.6275.

Wolbrecht, Eric T, Vicky Chan, David J Reinkensmeyer, and James E Bobrow. 2008. “Optimizing Compliant, Model-Based Robotic Assistance to Promote Neurorehabilitation.” *IEEE Transactions on Neural Systems and Rehabilitation Engineering : A Publication of the IEEE Engineering in Medicine and Biology Society* 16 (3): 286–97. doi:10.1109/TNSRE.2008.918389.

APPENDIX

Rigidity

The Logistic Function, which ranges from y = 0 to y = R:

$$f(\dot{q}) = \frac{R}{1 + e^{C(\dot{q} - \dot{q}_0)}}$$

where W is the maximum of the sigmoid curve, C controls the slope, and τ_0 is the midpoint of the curve. We want a curve that ranges from –W to W and is centered at 0. To shift the curve to the correct position, we set τ_0 to 0, double the range of the curve and subtracting half of the maximum, so that instead of a curve on the interval (0,W) we have a curve on the interval (-W,W):

$$f(\dot{q}) = \frac{2R}{1 + e^{C\dot{q}}} - R$$

Rearranging, we get:

$$f(\dot{q}) = R\left(\frac{1 - e^{C\dot{q}}}{1 + e^{C\dot{q}}}\right)$$

Finally, we want our resistive torque to act in the opposite direction of our movement, so we flip the sigmoid by making it negative:

$$f(\dot{q}) = -R\left(\frac{1 - e^{C\dot{q}}}{1 + e^{C\dot{q}}}\right)$$

Spasticity

The Chi-Squared cumulative density function for k degrees of freedom and t > 0 is as follows:

$$f(t;k) = \frac{t^{\left(\frac{k}{2}-1\right)}e^{-\frac{t}{2}}}{2^{\frac{k}{2}}\Gamma\left(\frac{k}{2}\right)}$$

We set k = 3 because it qualitatively produced the shape that we were looking for. This gives us:

$$f(t) = \frac{t^{\left(\frac{3}{2}-1\right)}e^{-\frac{t}{2}}}{2^{\frac{3}{2}}\Gamma\left(\frac{3}{2}\right)}$$

To reduce the number of constants, a “time scaling factor” (C_t) and a “magnitude scaling factor” (C_m) were calculated prior to each simulation. The C_t is responsible for modifying the duration of the chi-squared function such that it reaches three standard-deviations from the mean at time T. The C_m is responsible for normalizing the function to its peak value, which occurs at x = 1, so that later multiplying it by the maximal spasm magnitude, S, will scale the resultant torque appropriately. Chi2pdf() and chi2inv() refer to MATLAB functions for the Chi-squared probability distribution function and inverse cumulative distribution function, respectively:

$$C_t = chi2inv(0.99,3)/T$$

$$C_m = \frac{1}{chi2pdf(1,3) * 2^{\frac{3}{2}} * \Gamma\left(\frac{3}{2}\right)}$$

Using our definition for C_m, we can rewrite our function as:

$$f(t) = C_m t^{\frac{3}{2}-1} e^{-\frac{t}{2}} = C_m e^{-\frac{t}{2}} \sqrt{t}$$

And, in order to rescale the variable "t" to our desired duration, we multiply all instances of it by C_t:

$$f(t) = C_m e^{-\frac{tC_t}{2}} \sqrt{tC_t}$$

Finally, in order to avoid numerical instabilities introduced by MATLAB's ordinary differential equation solver jumping back to time values before the start of the spasm, we added a small constant to the values inside the square root:

$$f(t) = C_m e^{-\frac{tC_t}{2}} \sqrt{tC_t + 10^{-3}}$$

Weakness

We follow the same procedure we did for our rigidity model, using τ instead of $\dot{q}$ and W instead of R:

$$f(\tau) = W\left(\frac{1 - e^{C\tau}}{1 + e^{C\tau}}\right)$$

We want to set C so that the slope, or the first derivative, at 0 is equal to 1:

$$\frac{df(\tau)}{d\tau} = W\left(\frac{(1 + e^{C\tau})(-Ce^{C\tau}) - (1 - e^{C\tau})(Ce^{C\tau})}{(1 + e^{C\tau})^2}\right)$$

$$\frac{df(0)}{d\tau} = W\left(\frac{(1 + 1)(-C) - (1 - 1)(C)}{(1 + 1)^2}\right) = -\frac{2WC}{4} = 1$$

$$C = -\frac{2}{W}$$

VITA

NAME:	Joseph Robert Lancaster
EDUCATION:	B.A. Biology, Washington University in Saint Louis, St. Louis, Missouri 2009
TEACHING:	Teaching Assistant, Department of Bioengineering, University of Illinois at Chicago, Chicago, Illinois: Models of the Nervous System, 2012
HONORS:	Summer Undergraduate Research Fellowship, Washington University in St. Louis, 2007
PROFESSIONAL MEMBERSHIP:	Society for Neuroscience Engineering in Medicine and Biology Society
ABSTRACTS:	Lancaster, J., Wright, Z., Huang, F.C., and Patton, J.: The Effects of Motor Impairments on Movement Disorders. Conf. Proc. IEEE Eng. Med. Biol. Soc. 2014. Lancaster, J., Huang, F.C., and Patton, J.: Inverse Identification of Motor Deficits Using Movement Distributions and Mixtures of Expert Models. 45th Annual Meeting of the Society for Neuroscience. 2015.
PUBLICATIONS:	Lancaster, J., Johnston, J., Kappel, J., and Funk, C.: Design of Therapy for Rhesus Monkey Liver. UIC Bioengineering Student Journal. 3, no. 1 (2011): 45:49.